

Gluon Densities and Dihadron correlations

Bo-Wen Xiao

Penn State

- F. Dominguez, BX and F. Yuan, Phys.Rev.Lett.106:022301,2011.
- F. Dominguez, C. Marquet, BX and F. Yuan, arXiv:1101.0715[hep-ph].
- A. Stasto, BX and F. Yuan, in preparation.

Drell-Yan workshop at BNL, May, 2011

PENNSTATE



Outline

- 1 The effective k_t factorization
- 2 Gluon Distributions
 - DIS dijet
 - γ +Jet in pA
 - Gluon+Jet in pA
- 3 Phenomenology: Dihadron correlations at RHIC and future EIC
 - Dihadron correlations at RHIC
- 4 Conclusion and Outlook

The effective k_t factorization

For pA (dilute-dense system) collisions, there is an effective k_t factorization. The effective k_t factorization for pA (dilute-dense system) collisions for **back-to-back** dijets productions

$$\frac{d\sigma^{pA \rightarrow qfX}}{d^2k_{1\perp} d^2k_{2\perp} dy_1 dy_2} = x_p q(x_p, \mu^2) x f(x, q_{\perp}^2) \frac{1}{\pi} \frac{d\hat{\sigma}}{d\hat{t}}.$$

Remarks:

- **Penalty:** K_t dependent Parton distributions $x f(x, q_{\perp}^2)$ are not universal. $x f(x, q_{\perp}^2)$ here can be the quark or gluon distributions of the dense target.
- $x_p q(x_p, \mu^2)$ is the Feynman parton distribution of the dilute projectile.
- Thanks to the nuclear enhancement, soft gluon exchange from the dilute proton can be neglected.
- For pp , AA collisions, there is no such effective k_t factorization [Rogers, Mulders; 10].
- Disclaimer: The calculation is only done in the leading order (α_s and $\frac{q_{\perp}^2}{p_{\perp}^2}$) for a dense target without small- x evolution (such as BFKL or Balitsky-Kovchegov or JIMWLK equations). ([Dominguez, Mueller, Munier, Xiao, in preparation]).
- Assuming small- x limit, namely, $s \rightarrow \infty$, fixed Q^2 , $x \rightarrow 0$.

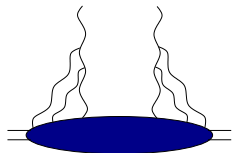
A Tale of Two Gluon Distributions

In small- x physics, two gluon distributions are widely used:

I. **Weizsäcker Williams** gluon distribution (**MV model**):

$$xG^{(1)} = \frac{S_{\perp}}{\pi^2 \alpha_s} \frac{N_c^2 - 1}{N_c} \Leftrightarrow$$

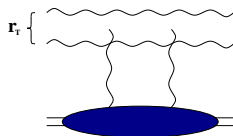
$$\times \int \frac{d^2 r_{\perp}}{(2\pi)^2} \frac{e^{-ik_{\perp} \cdot r_{\perp}}}{r_{\perp}^2} \left(1 - e^{-\frac{r_{\perp}^2 \rho_s^2}{2}} \right)$$



II. **Color Dipole** gluon distributions:

$$xG^{(2)} = \frac{S_{\perp} N_c}{2\pi^2 \alpha_s} \Leftrightarrow$$

$$\times \int \frac{d^2 r_{\perp}}{(2\pi)^2} e^{-ik_{\perp} \cdot r_{\perp}} \nabla_{r_{\perp}}^2 N(r_{\perp})$$



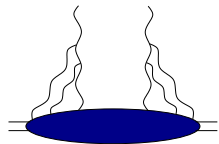
Remarks:

- The WW gluon distribution simply counts the number of gluons.
- The Color Dipole gluon distribution often appears in calculations. $N(r_{\perp})$ is the color dipole amplitude. It is now in fundamental representation. The adjoint representation form is similar and also widely used.
- Does this mean that gluon distributions are non-universal? Answer: **Yes** and **No!**
- These two distributions are used in R_{pA} calculation. [Kharzeev, Kovchegov, Tuchin; 03].

A Tale of Two Gluon Distributions

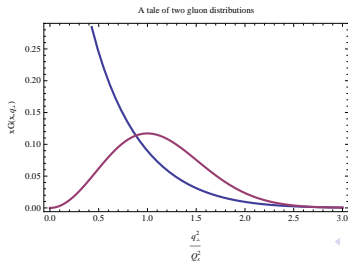
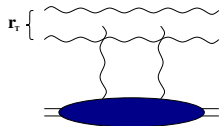
I. Weizsäcker Williams gluon distribution (MV model):

$$xG^{(1)} = \frac{S_{\perp}}{\pi^2 \alpha_s} \frac{N_c^2 - 1}{N_c} \Leftrightarrow \int \frac{d^2 r_{\perp}}{(2\pi)^2} \frac{e^{-ik_{\perp} \cdot r_{\perp}}}{r_{\perp}^2} \left(1 - e^{-\frac{r_{\perp}^2 Q_s^2}{2}} \right)$$



II. Color Dipole gluon distributions:

$$xG^{(2)} = \frac{S_{\perp} N_c}{2\pi^2 \alpha_s} \Leftrightarrow \int \frac{d^2 r_{\perp}}{(2\pi)^2} e^{-ik_{\perp} \cdot r_{\perp}} \nabla_{r_{\perp}}^2 N(r_{\perp})$$



A Tale of Two Gluon Distributions

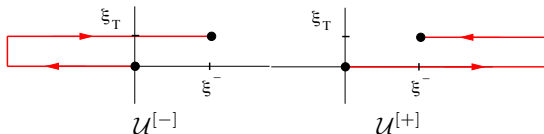
In terms of operators, we find these two gluon distributions can be defined as follows:
[Bomhof, Mulders and Pijlman; 06],[F. Dominguez, BX and F. Yuan, 11]

I. **Weizsäcker Williams** gluon distribution:

$$xG^{(1)} = 2 \int \frac{d\xi^- d\xi_\perp}{(2\pi)^3 P^+} e^{ixP^+ \xi^- - ik_\perp \cdot \xi_\perp} \text{Tr} \langle P | F^{+i}(\xi^-, \xi_\perp) \mathcal{U}^{[+] \dagger} F^{+i}(0) \mathcal{U}^{[+]} | P \rangle.$$

II. **Color Dipole** gluon distributions:

$$xG^{(2)} = 2 \int \frac{d\xi^- d\xi_\perp}{(2\pi)^3 P^+} e^{ixP^+ \xi^- - ik_\perp \cdot \xi_\perp} \text{Tr} \langle P | F^{+i}(\xi^-, \xi_\perp) \mathcal{U}^{[-] \dagger} F^{+i}(0) \mathcal{U}^{[+]} | P \rangle.$$



Remarks:

- The WW gluon distribution is the **conventional gluon distributions**. In light-cone gauge, it is the **gluon density**. (**Only final state interactions**.)
- The dipole gluon distribution has no such interpretation. (**Initial and final state interactions**.)
- Both definitions are gauge invariant.
- Same after integrating over q_\perp .

A Tale of Two Gluon Distributions

In terms of operators, we find these two gluon distributions can be defined as follows:

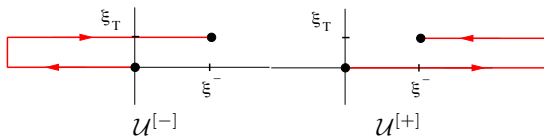
[Bomhof, Mulders and Pijlman; 06],[F. Dominguez, BX and F. Yuan, 11]

I. **Weizsäcker Williams** gluon distribution (Easy to evaluate in the MV model):

$$xG^{(1)} = 2 \int \frac{d\xi^- d\xi_\perp}{(2\pi)^3 P^+} e^{ixP^+ \xi^- - ik_\perp \cdot \xi_\perp} \text{Tr} \langle P | F^{+i}(\xi^-, \xi_\perp) \mathcal{U}^{[+] \dagger} F^{+i}(0) \mathcal{U}^{[+]} | P \rangle.$$

II. **Color Dipole** gluon distributions:

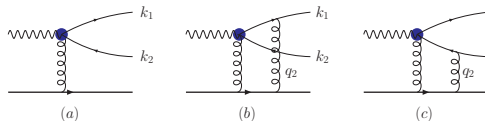
$$xG^{(2)} = 2 \int \frac{d\xi^- d\xi_\perp}{(2\pi)^3 P^+} e^{ixP^+ \xi^- - ik_\perp \cdot \xi_\perp} \text{Tr} \langle P | F^{+i}(\xi^-, \xi_\perp) \mathcal{U}^{[-] \dagger} F^{+i}(0) \mathcal{U}^{[+]} | P \rangle.$$



Questions:

- Can we distinguish these two gluon distributions? **Yes, We Can.**
- How to measure $xG^{(1)}$ directly? **DIS dijet.**
- How to measure $xG^{(2)}$ directly? **DY or Direct γ +Jet in pA collisions.**
Maybe single-inclusive particle production in pA (Subtle).
- What happens in gluon+jet production in pA collisions? **It's complicated!**

DIS dijet



TMD factorization approach:

$$\frac{d\sigma^{\gamma_T^* A \rightarrow q\bar{q}+X}}{d\mathcal{P}.S.} = \delta(x_{\gamma^*} - 1) x_g G^{(1)}(x_g, q_\perp) H_{\gamma_T^* g \rightarrow q\bar{q}}, \quad \text{with } d\mathcal{P}.S. = dy_1 dy_2 d^2 P_\perp d^2 q_\perp.$$

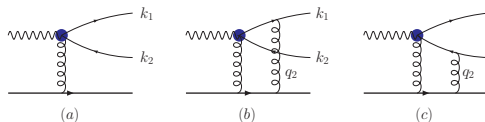
Dipole model approach: $S_{x_g}^{(4)}(x, b; b', x') = \frac{1}{N_c} \langle \text{Tr} U(x) U^\dagger(x') U(b') U^\dagger(b) \rangle_{x_g}$ **Quadrupole**

$$\begin{aligned} \frac{d\sigma^{\gamma_T^* A \rightarrow q\bar{q}+X}}{d\mathcal{P}.S.} &\propto N_c \alpha_{em} e_q^2 \int \frac{d^2 x}{(2\pi)^2} \frac{d^2 x'}{(2\pi)^2} \frac{d^2 b}{(2\pi)^2} \frac{d^2 b'}{(2\pi)^2} e^{-ik_{1\perp} \cdot (x-x')} \\ &\times e^{-ik_{2\perp} \cdot (b-b')} \sum \psi_T^*(x-b) \psi_T(x'-b') \\ &\left[1 + S_{x_g}^{(4)}(x, b; b', x') - S_{x_g}^{(2)}(x, b) - S_{x_g}^{(2)}(b', x') \right], \end{aligned}$$

Two independent calculations agree perfectly in the correlation limit (Large P_\perp and Small q_\perp).

DIS dijet

The dijet production in DIS.



TMD factorization approach:

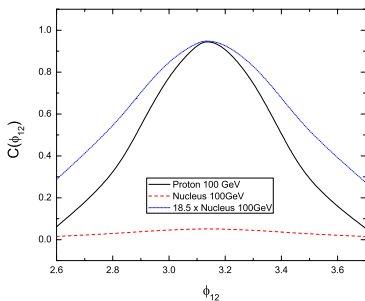
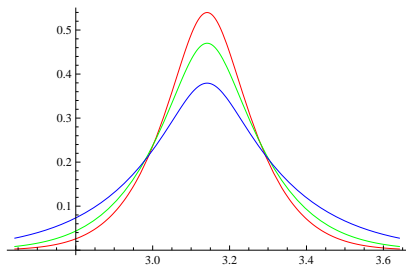
$$\frac{d\sigma^{\gamma_T^* A \rightarrow q\bar{q}+X}}{d\mathcal{P}.S.} = \delta(x_{\gamma^*} - 1) x_g G^{(1)}(x_g, q_{\perp}) H_{\gamma_T^* g \rightarrow q\bar{q}},$$

Remarks:

- Dijet in DIS is the **only physical** process which can measure **Weizsäcker Williams** gluon distributions.
- **Golden measurement** for the **Weizsäcker Williams** gluon distributions of nuclei at small-x. The cross section is directly related to the WW gluon distribution.
- **EIC** will provide us a **perfect machine** to study the strong gluon fields in nuclei.

DIS dijet correlation

Azimuthal angle correlation of dijet in DIS probes the **WW** gluon distributions

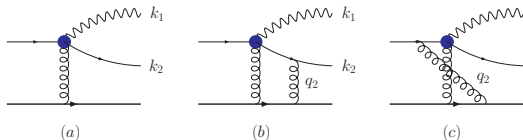


Remarks:

- $k_{1\perp} = 5.5 \text{ GeV}$, $k_{2\perp} = 5.0 \text{ GeV}$ and $Q_s^2 = 1, 1.5, 3 \text{ GeV}^2$;
- Only away side peak is plotted due to the correlation limit.
- **Suppression** of away side peak and **increase of width** at large Q_s^2 .
- Dramatic change between ep and eA collisions. $Q_s^2 = 4 \text{ GeV}^2$, $z_{h1} = z_{h2} = 0.3$, $2 \text{ GeV} < p_{1\perp} < 3 \text{ GeV}$ and $1 \text{ GeV} < p_{2\perp} < 2 \text{ GeV}$.
- No pedestal.

γ +Jet in pA collisions

The direct photon + jet production in pA collisions. (Drell-Yan Process follows the same factorization.)



TMD factorization approach:

$$\frac{d\sigma^{(pA \rightarrow \gamma q + X)}}{d\mathcal{P} \cdot \mathcal{S}} = \sum_f x_1 q(x_1, \mu^2) x_g G^{(2)}(x_g, q_\perp) H_{qg \rightarrow \gamma q}.$$

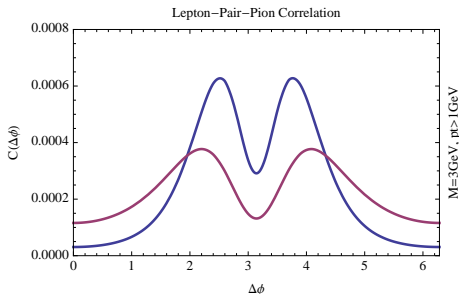
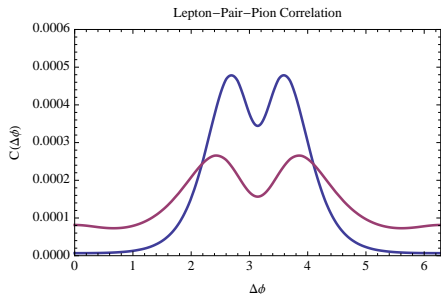
Remarks:

- Independent CGC calculation gives the identical result in the correlation limit.
- This process can be calculated exactly for all range of azimuthal angles.
- Direct measurement of the **Color Dipole** gluon distribution.
- The RHIC and future LHC experiments shall provide us some information on this.

Dilepton Pair + hadron correlation

[F. Dominguez, BX and F. Yuan, in preparation]

Azimuthal angle correlation of $\gamma^* + \pi^0$ at forward rapidity 3.2:



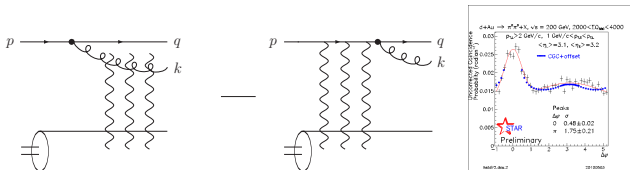
Remarks:

- $p_{1\perp} > 1.5\text{GeV}$, $p_{2\perp} > 1.5\text{GeV}$ and $M^2 = 1\text{GeV}^2$;
- $p_{1\perp} > 1\text{GeV}$, $p_{2\perp} > 1\text{GeV}$ and $M^2 = 9\text{GeV}^2$;
- Suppression of away side peak at central dAu collisions.
- Double peak structure on the away side comes from the fact that $xG^{(2)} \propto q_{\perp}^2$ in the small q_{\perp} limit.

Existing calculations on dijet production

Let us first look back, and re-examine the existing calculations on dijet productions.

I. Quark+Gluon channel [Marquet, 07] and [Albacete, Marquet, 10]



- Prediction of saturation physics.
- All the framework is correct, but over-simplified 4-point function.
- Improvement [F. Dominguez, C. Marquet, BX and F. Yuan, 11.]

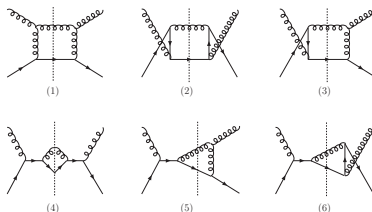
$$S_{x_g}^{(4)}(x_1, x_2; x'_2, x'_1) \simeq e^{-\frac{C_F}{2} [\Gamma(x_1 - x_2) + \Gamma(x'_2 - x'_1)]} \\ - \frac{F(x_1, x_2; x'_2, x'_1)}{F(x_1, x'_2; x_2, x'_1)} \left(e^{-\frac{C_F}{2} [\Gamma(x_1 - x_2) + \Gamma(x'_2 - x'_1)]} - e^{-\frac{C_F}{2} [\Gamma(x_1 - x'_1) + \Gamma(x'_2 - x_2)]} \right)$$

II. Gluon+Gluon channel [Tuchin, 09]

- Fit the RHIC data amazingly well.
- Not correct, since the starting formula is K_T factorization formula.

Gluon+Jet in pA collisions

Gluon+Jet in pA collisions is the **dominant** channel for dijet production. For quark+gluon channel in the **TMD approach**, we have the following hard cross sections:

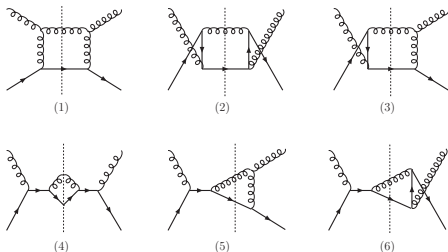


Hard cross sections and Color factors:

(1)	(2)	(3)	(4)	(5)	(6)
$-\frac{4(\hat{t}^2 - \hat{s}\hat{u})^2}{\hat{t}^2 \hat{s}\hat{u}}$	$-\frac{2(\hat{u}^2 + \hat{t}^2)}{\hat{s}\hat{u}}$	$\frac{2(\hat{t}^2 - \hat{s}\hat{u})(\hat{u} - \hat{t})}{\hat{s}\hat{t}\hat{u}}$	$-\frac{2(\hat{s}^2 + \hat{t}^2)}{\hat{s}\hat{u}}$	$-\frac{2(\hat{t}^2 - \hat{s}\hat{u})(\hat{s} - \hat{t})}{\hat{s}\hat{t}\hat{u}}$	$\frac{2\hat{t}^2}{\hat{s}\hat{u}}$
$\frac{1}{2}$	$\frac{C_F}{2N_c}$	$-\frac{1}{4}$	$\frac{C_F}{2N_c}$	$\frac{1}{4}$	$-\frac{1}{4N_c^2}$

Gluon+Jet in pA collisions

For quark+gluon channel in the **TMD approach**, different graph corresponds to different gluon distributions: [Bomhof, Mulders and Pijlman; 06]



$$\Phi_g^{(1)} = \left\langle \text{Tr} \left[F(\xi) \left\{ \frac{1}{2} \frac{\text{Tr} [\mathcal{U}[\square]]}{N_c} \mathcal{U}^{[+]\dagger} + \frac{1}{2} \mathcal{U}^{[-]\dagger} \right\} F(0) \mathcal{U}^{[+]} \right] \right\rangle,$$

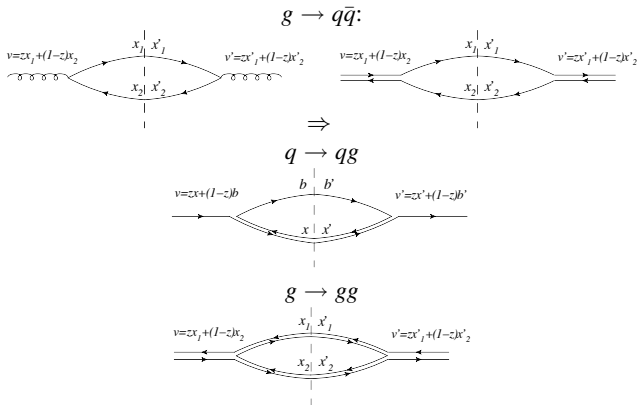
$$\Phi_g^{(2)} = \left\langle \text{Tr} \left[F(\xi) \left\{ \frac{N_c^2}{N_c^2 - 1} \frac{\text{Tr} [\mathcal{U}[\square]]}{N_c} \mathcal{U}^{[+]\dagger} - \frac{1}{N_c^2 - 1} \mathcal{U}^{[-]\dagger} \right\} F(0) \mathcal{U}^{[+]} \right] \right\rangle,$$

$$\Phi_g^{(3)} = \left\langle \text{Tr} \left[F(\xi) \frac{\text{Tr} [\mathcal{U}[\square]]}{N_c} \mathcal{U}^{[+]\dagger} F(0) \mathcal{U}^{[+]} \right] \right\rangle,$$

$$\Phi_g^{(4),(5),(6)} = \left\langle \text{Tr} \left[F(\xi) \mathcal{U}^{[-]\dagger} F(0) \mathcal{U}^{[+]} \right] \right\rangle.$$

Large N_c limit

Graphical representation of dijet processes in the large N_c limit



Two fundamental building blocks.

Gluon+quark jets correlation

Including all the $qg \rightarrow qg$, $gg \rightarrow gg$ and $gg \rightarrow q\bar{q}$ channels, a lengthy calculation gives

$$\begin{aligned} \frac{d\sigma^{(pA \rightarrow \text{Dijet}+X)}}{d\mathcal{P} \cdot \mathcal{S}} &= \sum_q x_1 q(x_1, \mu^2) \frac{\alpha_s^2}{\hat{s}^2} \left[\mathcal{F}_{qg}^{(1)} H_{qg}^{(1)} + \mathcal{F}_{qg}^{(2)} H_{qg}^{(2)} \right] \\ &+ x_1 g(x_1, \mu^2) \frac{\alpha_s^2}{\hat{s}^2} \left[\mathcal{F}_{gg}^{(1)} \left(H_{gg \rightarrow q\bar{q}}^{(1)} + \frac{1}{2} H_{gg \rightarrow gg}^{(1)} \right) \right. \\ &\left. + \mathcal{F}_{gg}^{(2)} \left(H_{gg \rightarrow q\bar{q}}^{(2)} + \frac{1}{2} H_{gg \rightarrow gg}^{(2)} \right) + \mathcal{F}_{gg}^{(3)} \frac{1}{2} H_{gg \rightarrow gg}^{(3)} \right], \end{aligned}$$

with the various gluon distributions defined as

$$\begin{aligned} \mathcal{F}_{qg}^{(1)} &= xG^{(2)}(x, q_\perp), \quad \mathcal{F}_{qg}^{(2)} = \int xG^{(1)} \otimes F, \\ \mathcal{F}_{gg}^{(1)} &= \int xG^{(2)} \otimes F, \quad \mathcal{F}_{gg}^{(2)} = - \int \frac{q_{1\perp} \cdot q_{2\perp}}{q_{1\perp}^2} xG^{(2)} \otimes F, \\ \mathcal{F}_{gg}^{(3)} &= \int xG^{(1)}(q_1) \otimes F \otimes F, \end{aligned}$$

where $F = \int \frac{d^2 r_\perp}{(2\pi)^2} e^{-iq_\perp \cdot r_\perp} \frac{1}{N_c} \langle \text{Tr} U(r_\perp) U^\dagger(0) \rangle_{x_g}$.

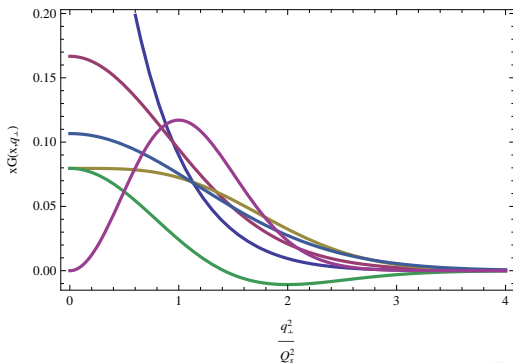
Remarks: Only the term in NavyBlue color was known before.

Illustration of gluon distributions

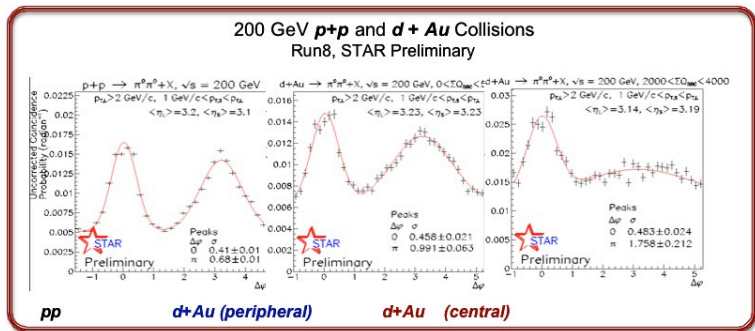
The various gluon distributions:

$$\begin{aligned}
 & xG_{\text{WW}}^{(1)}(x, q_{\perp}), \quad \mathcal{F}_{qg}^{(1)} = xG^{(2)}(x, q_{\perp}), \\
 \mathcal{F}_{gg}^{(1)} &= \int xG^{(2)} \otimes F, \quad \mathcal{F}_{gg}^{(2)} = - \int \frac{q_{1\perp} \cdot q_{2\perp}}{q_{1\perp}^2} xG^{(2)} \otimes F, \\
 \mathcal{F}_{gg}^{(3)} &= \int xG^{(1)}(q_1) \otimes F \otimes F, \quad \mathcal{F}_{qg}^{(2)} = \int xG^{(1)} \otimes F
 \end{aligned}$$

6 different gluon distributions



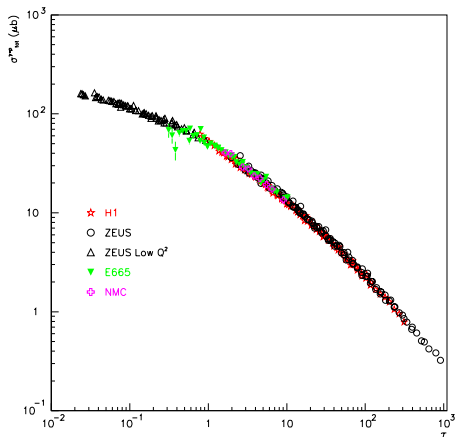
STAR measurement on di-hadron correlation in dA collisions



- There is no sign of suppression in the $p + p$ and $d + Au$ peripheral data.
- The suppression and broadening of the away side jet in $d + Au$ central collisions is due to the multiple interactions between partons and dense nuclear matter (**CGC**).
- Dissect the data into three features:
Width σ of peaks, Pedestal P and Peak suppression.
- Near side peak: maybe due to 2-hadron fragmentation.

Golec-Biernat Wusthoff model and Geometrical Scaling

[Golec-Biernat, Wusthoff,; 98], [Golec-Biernat, Stasto, Kwiecinski; 01]



- Use Golec-Biernat Wusthoff model for the saturation momentum, $Q_s^2(x) = Q_{s0}^2(x/x_0)^{-\lambda}$ with $Q_{s0} = 1\text{GeV}$, $x = 3.04 \times 10^{-3}$ and $\lambda = 0.288$.
- All data of $\sigma_{tot}^{\gamma^*p}$ when $x \leq 0.01$ and $Q^2 \leq 450\text{GeV}^2$ plotting as function of $\tau = Q^2/Q_s^2$ falls on a curve.

The forward dihadron correlations in dAu collisions at RHIC

Measurement: For the process $dAu \rightarrow h_1 h_2 X$ at $\sqrt{s} = 200\text{GeV}$, both STAR and PHENIX measure the coincidence probability ($x_g = x_1 e^{-y_1} + x_2 e^{-y_2}$ and $x_d = x_1 e^{y_1} + x_2 e^{y_2}$)

$$C(\Delta\phi) = \frac{N_{\text{pair}}(\Delta\phi)}{N_{\text{trig}}}$$

where $N_{\text{pair}}(\Delta\phi)$ is the yield of two forward π^0 which includes a trigger particle with a transverse momentum $p_{1\perp}^{\text{trig}} > 2\text{GeV}$ and an associate particle with $p_{1\perp}^{\text{trig}} > p_{2\perp}^{\text{assoc}} > 1\text{GeV}$.

Calculation: In terms of theory, this coincidence probability can be calculated via

$$C(\Delta\phi) = \frac{\int_{|p_{1\perp}|, |p_{2\perp}|} \frac{d\sigma_{\text{Correlated}}}{dy_1 dy_2 d^2p_{1\perp} d^2p_{2\perp}} + \int_{|p_{1\perp}|, |p_{2\perp}|} \frac{d\sigma_{\text{Uncorrelated}}}{dy_1 dy_2 d^2p_{1\perp} d^2p_{2\perp}}}{\int_{|p_{1\perp}|} \frac{d\sigma_{\text{Single Inclusive}}}{dy_1 d^2p_{1\perp}}}$$

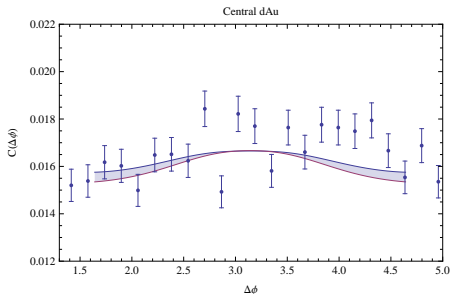
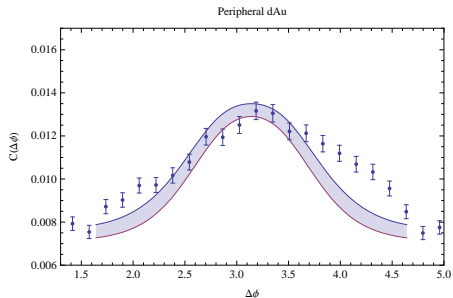
Remarks:

- $\sigma_{\text{Correlated}}$ gives the peaks.
- $\sigma_{\text{Uncorrelated}}$ gives the pedestal (offset). \Leftarrow two (or more) independent single scatterings. [Strikman, Vogelsang; 11]
- $\sigma_{\text{Single Inclusive}}$ matches the single inclusive cross section in forward dAu collisions.
- **Data Dissection:** Width σ of peaks, Pedestal P and peak suppression.
- Width σ of peaks and Pedestal $P \uparrow$, while peak \downarrow with $Q_s \uparrow$. Why?

Comparing to STAR data

[A. Stasto, BX, F. Yuan, in preparation]

For away side peak in both **peripheral** and **central** dAu collisions in $q + g$ channel:

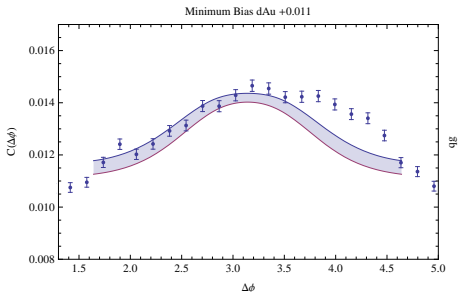


- The framework does not work for pp since the saturation scale Q_s is too low at $\sqrt{s} = 200\text{GeV}$.
- Use Golec-Biernat Wusthoff model for the saturation momentum, $Q_s^2(x) = Q_{s0}^2(x/x_0)^\lambda$; Adding the nuclear and impact factor dependence: $Q_{sA}^2 = c(b)A^{1/3}Q_s^2(x)$ with $c(b) \propto \sqrt{1 - b^2/R^2}$.
- Peripheral $b = 6.8 \pm 1.7\text{fm}$ with $c(b) = 0.45$ and width $\sigma \simeq 0.99$;
- Central $b = 2.7 \pm 1.3\text{fm}$ with $c(b) = 0.85$ and width $\sigma \simeq 1.6$.

Comparing to STAR data

[A. Stasto, BX, F. Yuan, in preparation]

For minimum bias away side peak in dAu collisions in $q + g$ channel:



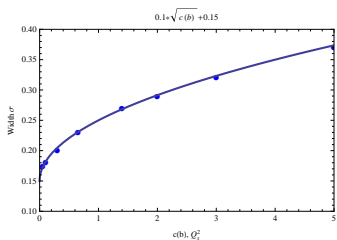
- Peripheral $b = 6.8 \pm 1.7\text{fm}$ with $c(b) = 0.45$ and width $\sigma \simeq 0.99$;
- Central $b = 2.7 \pm 1.3\text{fm}$ with $c(b) = 0.85$ and width $\sigma \simeq 1.6$;
- Minimum Bias $c(b) = 0.56 \Rightarrow \langle b \rangle = 6\text{fm}$ and width $\sigma \simeq 1.2$.

The connection between the Width σ of away side peaks and $Q_{sA}^2(b)$

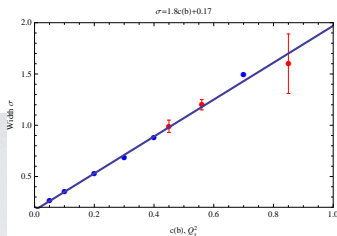
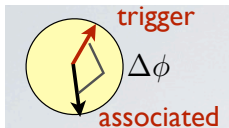
Let us do a simple exercise first. Assume the relevant gluon distribution has the form $\exp(-\frac{q_\perp^2}{Q_s^2(b)})$ with $q_\perp = k_{1\perp} + k_{2\perp}$, thus around the away side peaks

$$C(\Delta\phi) \propto \exp\left[-\frac{(|k_{1\perp}| - |k_{2\perp}|)^2 + 2|k_{1\perp}||k_{2\perp}|(1 + \cos\Delta\phi)}{Q_{sA}^2(b)}\right]$$

$$\propto \exp\left[-\frac{|k_{1\perp}||k_{2\perp}|(\Delta\phi - \pi)^2}{Q_{sA}^2(b)}\right] \Rightarrow \sigma \propto \frac{Q_{sA}(b)}{\Lambda} \propto \sqrt{c(b)}$$



eA collisions



dAu collisions

- However, we found $\sigma \propto c(b) \propto \frac{Q_{sA}^2(b)}{\Lambda^2}$ from dAu data. (No additional parameter!)
- $C(\Delta\phi) \propto C_1 + C_2 \int(\frac{q_\perp^2}{Q_s^2}) + C_3 \int(\frac{q_\perp^2}{Q_s^2})^2$ with $C_2 \simeq 0$

Comparing to STAR data

[A. Stasto, BX, F. Yuan, in preparation]

Assume that the pedestal (offset) mostly comes from two independent single scatterings (**double parton scattering**[Strikman, Vogelsang; 11]):

$$P = \frac{\int_{|p_{1\perp}|} \frac{dN_{\text{Single Inclusive}}}{dy_1 d^2 p_{1\perp}} \times \int_{|p_{2\perp}|} \frac{dN_{\text{Single Inclusive}}}{dy_2 d^2 p_{2\perp}}}{\int_{|p_{1\perp}|} \frac{dN_{\text{Single Inclusive}}}{dy_1 d^2 p_{1\perp}}}$$

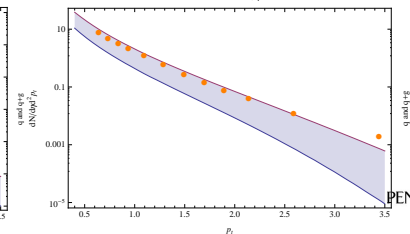
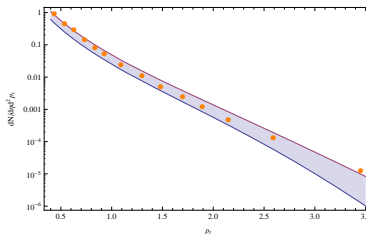
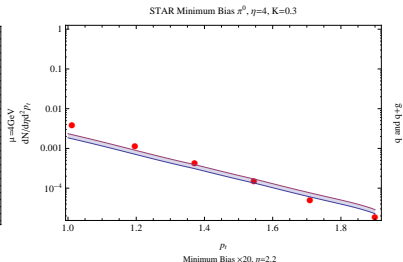
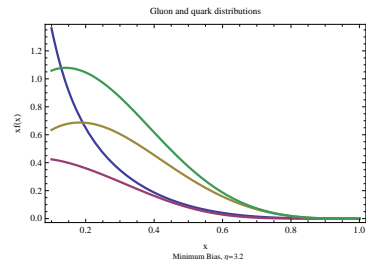
with $\frac{dN_{\text{Single Inclusive}}}{dy d^2 p_{\perp}} = \int dz x q(x_p) F_{x_g}(k_{\perp}) D(z)$

- The pedestal increase as the saturation momentum increases.
- Multiple parton interactions? Three?

Offsets	Exp	Theory $q + g$	Theory $q + g$ and $g + g$
Peripheral	0.007 ± 0.001	0.0065	0.016
Central	0.015 ± 0.001	0.011	0.018

$q + g$ channel as compared to $g + g$ channel

At ($\eta \simeq 4$), the **quark** distribution dominates the $\sigma_{\text{Single Inclusive}}$. Not true, for $\eta \simeq 3.2$ or 2.2.
STAR dAu π^0 data and **BRAHMS h^- data** (80 percent of h^- is π^-)



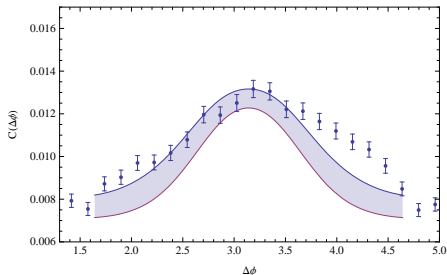
Comment: The **height of away side peak** is very sensitive to the value of total single inclusive cross section.

Comparing to STAR data including both $q + g$ and $g + g$

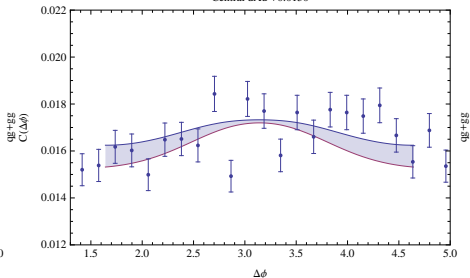
[A. Stasto, BX, F. Yuan, in preparation]

For away side peak in both **peripheral** and **central** dAu collisions:

Peripheral $dAu +0.007$



Central $dAu +0.0150$

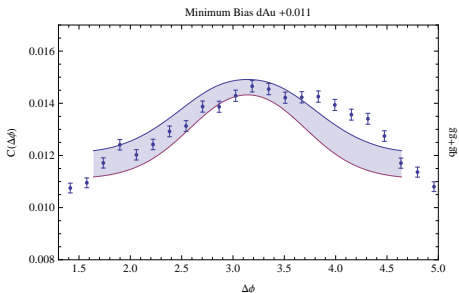


- Adding a k -factor of 2 to the ratio since the total single inclusive cross section is twice of the data at $\eta = 3.2$.
- Other parameters are kept the same.

Comparing to STAR data including both $q + g$ and $g + g$

[A. Stasto, BX, F. Yuan, in preparation]

For minimum bias away side peak in dAu collisions in $q + g$ channel:



- Adding a k -factor of 2 to the ratio since the total single inclusive cross section is twice of the data at $\eta = 3.2$.
- Peripheral $b = 6.8 \pm 1.7\text{fm}$ with $c(b) = 0.45$ and width $\sigma \simeq 0.99$;
- Central $b = 2.7 \pm 1.3\text{fm}$ with $c(b) = 0.85$ and width $\sigma \simeq 1.6$;
- Minimum Bias $c(b) = 0.56 \Rightarrow \langle b \rangle = 6\text{fm}$ and width $\sigma \simeq 1.2$.

Conclusion and Outlook

- The effect of the k_t factorization violation is **calculable and resumable**. This eventually helps us to reach an effective factorization for the collisions between a dilute projectile and a dense target.
- DIS dijet provides **direct information** of the WW gluon distributions. **Perfect** for testing CGC, and ideal measurement for EIC.
- Parton distributions may not be exactly universal, but they are related.

	Inclusive	Single Inc	DIS dijet	γ +jet	g+jet
$xG^{(1)}$	×	×	√	×	√
$xG^{(2)}, F$	√	√	×	√	√

× \Rightarrow Do Not Appear. √ \Rightarrow Appear.

- **Two fundamental gluon distributions**. Other gluon distributions are just different **combinations and convolutions** of these two.
- Dilepton-pair-hadron correlations probes the **dipole gluon distribution**.
- Dihadron correlation calculation and comparison with the STAR data.